Journal of Cellular and Molecular Medicine
A JOURNAL OF TRANSLATIONAL MEDICINE

J. Cell. Mol. Med. Vol 15, No 12, 2011 pp. 2586-2593

Characterization of upper lamina propria interstitial cells in bladders from patients with neurogenic detrusor overactivity and bladder pain syndrome

Thomas Gevaert [a, b, *], Rita De Vos [a], Wouter Everaerts [b], Louis Libbrecht [c], Frank Van Der Aa [b], Joost van den Oord [a], Tania Roskams [a], Dirk De Ridder [b]

[a] *KU Leuven, Department of Morphology and Molecular Pathology, Leuven, Belgium*
[b] *KU Leuven, Department of Urology, University Hospitals Gasthuisberg, Leuven, Belgium*
[c] *UGent, Department of Pathology, Ghent, Belgium*

Received: September 26, 2010; Accepted: January 6, 2011

Abstract

The upper lamina propria (ULP) area of interstitial cells (IC) in bladder has been studied for more than a decade in several species including human beings. Nevertheless there is still lack of uniformity in terminology of this cell layer. The aim of the present study was to add new data to the morphological and immunohistochemical phenotype of these cells and to find out whether this phenotype is changed in bladders from patients with neurogenic detrusor overactivity (NDO) and bladder pain syndrome (BPS). Bladder tissue was obtained from a control group and from patients with NDO and BPS. Samples were processed for morphology, electron microscopy and immunohistochemistry. A morphological and immunohistochemical phenotype for the ULP IC was assessed and changes in this phenotype were looked for in samples from patients with NDO and BPS. The ULP IC were characterized ultrastructurally by the presence of actin filaments with densifications, many caveolae and abundant rough endoplasmic reticulum (RER); on immunohistochemistry ULP IC were immunoreactive for α-sma, vimentin, CD10 and podoplanin and categorized as interstitial Cajal-like cells (ICLC). In NDO and BPS bladders we found a phenotypical shift towards a fibroblastic phenotype which was even more pronounced in the NDO group. In both groups there was also an increased presence in ULP lymphocytes. The ULP area in the human bladder contains a population of ICLC with distinct ultrastructural morphology and immunohistochemical phenotype. Their unique α-sma$^+$/desmin$^-$/CD34$^-$ phenotype allows studying this population in various bladder disorders. In bladders form patients with BPS and NDO, we observed these ULP ICLC to shift towards a fibroblast phenotype.

Keywords: bladder • neurogenic detrusor overactivity • bladder pain syndrome • interstitial cell • myofibroblast • lamina propria

Introduction

The urinary bladder serves as reservoir that alternates between urine storage and efficient urine expulsion at a convenient moment. These apparently simple functions are regulated by a complex control system that is located in the bladder wall, the peripheral ganglia, the spinal cord and the brain. Recent insights into the complex morphological and functional organization of bladder wall, suggest that not only neuronal [1], but also non-neuronal (sensory and motor) pathways play a crucial role in bladder (dys)function [2].

One of the non-neuronal cells that is suggested to coordinate local bladder processes is the interstitial cell (IC). In recent years several independent groups have reported the presence of these cells in animal and human bladder (for review see [3–6]). These cells have mainly been described in the upper lamina propria (ULP, directly underneath the urothelium, sometimes called suburothelium) and the intermuscular spaces in the detrusor. In the ULP these cells have been categorized heterogeneously as interstitial Cajal-like cells (ICLC) [4, 7] or myofibroblasts [8, 9], which are by definition two different types of cells. Reasons for this diverse nomenclature are mainly the use of different experimental methods (electron microscopy *versus* light microscopy and immunohistochemistry) and the use of different tissue hosts

*Correspondence to: Thomas GEVAERT,
Department of Morphology and Molecular Pathology,
Minderbroedersstraat 12,
3000 Leuven, Belgium.
Tel.: 0032/16346930
Fax: 0032/16346931
E-mail: Thomas.Gevaert@uz.kuleuven.ac.be

doi: 10.1111/j.1582-4934.2011.01262.x

(human *versus* animals). A constant finding however is that these IC in the ULP are closely packed together, arranged in several consecutive layers and that these cells are immunoreactive for the intermediate filament vimentin.

Because of their particular organization just underneath the urothelium, ULP IC have attracted interest of many investigators because they could embody a structural and functional link between urothelial cells and sensory nerves and/or between urothelial cells and detrusor smooth muscle cells. Moreover these cells might be involved in the pathophysiology of functional bladder disorders, where local signalling processes are thought to play important roles. Two of the most frequent functional bladder disorders are neurogenic detrusor overactivity (NDO) and bladder pain syndrome (BPS). The aetiology of both pathologies is still far from being fully elucidated, but local alterations in the bladder wall are likely to be involved. In this paper, we studied the morphology of ULP IC in normal bladders and dysfunctional bladders from patients with NDO due to multiple sclerosis (MS) and BPS to describe the structural alterations that may disrupt normal bladder physiology.

Table 1 Table listing the antibodies used in the present study

Antibody	Manufacturer	Host	Clone	Titre
Vimentin	Dako, Glostrup, Denmark	Mouse	V9	1/500
α-sma	Dako	Mouse	1A4	1/200
Desmin	Dako	Mouse	D33	1/50
CD34	Dako	Mouse	QBEnd 10	1/100
CD10	Dako	Mouse	56C6	1/50
Podoplanin	Dako	Mouse	D2–40	1/50
C-kit	Dako	Rabbit	/	1/750
Tryptase	Dako	Mouse	AA1	1/200
CD3	Dako	Rabbit	/	1/250
CD20	Dako	Mouse	L26	1/500
Synaptophysin	Dako	Mouse	SY38	1/50
Neurofilament	Dako	Mouse	2F11	1/40

Materials and methods

Patient selection

The study protocol was in accordance with EU guidelines and approved by the institution's ethical committee. All patients received information about the study and signed an informed consent file. To avoid gender bias only female patients were included, all aged between 30 and 55 years. Bladder tissue samples from patients with NDO (all patients with MS, at least 5 years after diagnosis, all having continence problems) and BPS (diagnosed by clinical symptoms and histopathology) were compared with tissue obtained from patients without evidence of bladder disease undergoing invasive procedures for ureteral stone disease. Each experimental group consisted of bladder samples from seven different patients.

Tissue sampling and processing

Bladder tissue was obtained with two different procedures. Cold cup biopsies were taken during endoscopic procedures (diagnostic hydrodistention or ureteroscopy), whereas *ex vivo* biopsies were taken from cystectomy specimens immediately after surgery. All bladder biopsies were taken from the bladder dome (non-trigonal regions). One part of a each bladder biopsy was immediately fixed in formalin 6% and subsequently embedded in paraffin, whereas the other part was prepared for electron microscopy.

Immunohistochemistry

From a series of consecutive sections, the first slide from each biopsy was routinely stained with haematoxylin and eosin to check the presence of urothelium, lamina propria and at least some muscular layers of the detrusor. For immunohistochemistry 5-μm-thick sections were deparaffinized in xylene, followed by rehydration. Before staining, heat-induced epitope retrieval was performed by incubating the sections in Tris-ethylenediaminetetraacetic acid buffer (pH 9.0) for 30 min. in a hot water bath at 98.5°C. Endogenous peroxidase activity was blocked using 0.3% H_2O_2 in methanol for 20 min. Sections were incubated with primary antibodies for 30 min. at room temperature, followed by incubation with a peroxidase-labelled polymer (DakoCytomation, Glostrup, Denmark) during 30 min. and a subsequent incubation with a substrate chromogen for another 15 min. In between each step, the sections were thoroughly rinsed in three changes of phosphate-buffered saline, pH 7.2. Nuclear counterstaining was done with haematoxylin. The primary antibodies used are listed in Table 1. The panel of antibodies was chosen to phenotype IC: vimentin for mesenchymal properties, α-sma and desmin for smooth muscle properties, c-kit and CD34 for ICC properties, CD10 and podoplanin for properties of activated fibroblasts, neurofilament for neural properties and synaptophysin for neuro-endocrine properties. The titres for the primary and secondary antibodies were determined during use for daily clinical immunohistochemistry in our lab. Negative controls consisted of omission of the primary antibody, resulting in absence of immunoreactivity. For all antibodies except CD20, CD3 and tryptase, internal positive controls in bladder tissue were present. To compare histological staining patterns serial sections were stained with different antibodies. Images were acquired using a Leica DM LB microscope equipped with a DC300FX camera (Leica Microsystems, Aartselaar, Belgium).

Electron microscopy

A small sample of each biopsy was fixed in fixed in 2.5% glutaraldehyde, 0.1 mol/l phosphate buffer at 4°C overnight. After 1 hr after fixation in 1% osmium tetroxide, 0.1mol/l phosphate buffer at 4°C, the samples were dehydrated in graded series of alcohol and embedded in epoxy resin. First semi-thin sections were made to check the presence of urothelium and lamina propria. Then ultra-thin sections 50 to 60 nm were cut from representative samples, stained with uranyl acetate and lead citrate and examined at 50 kV using a Zeiss EM 900 electron microscope (Carl Zeiss,

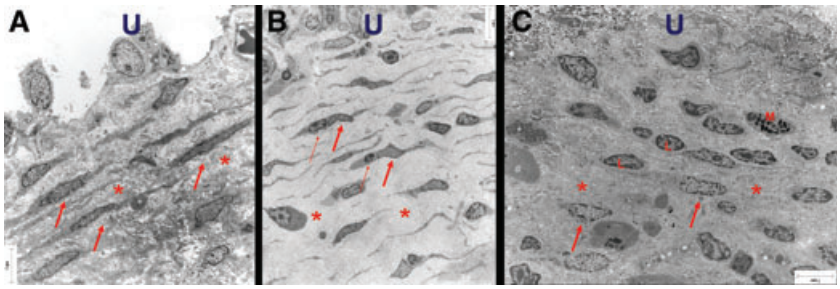

Fig. 1 Electron micrograph of ULP ICLC in control (**A**), NDO, (**B**) and BPS (**C**) bladders. (**A**) Many parallel layers of ICLC (arrows) embedded in a dense extracellular matrix (asterisk). (**B**) Multiple parallel layers of slender ICLC (thick arrow) often in close association with lymphocytes (thin arrow). Note the large intercellular space (asterisk) filled with less dense intercellular matrix components. (**C**) Fragmented layers of ICLC (arrows). Note the presence of lymphocytes (l) and mast cells (m). Dense extracellular matrix components are obvious (asterisk). Scale bars: 7 μm. U: urothelial area.

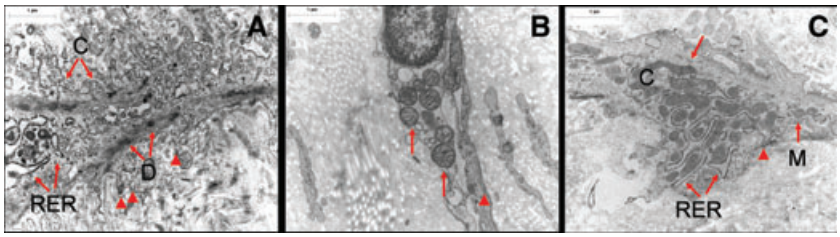

Fig. 2 Electron micrographs comparing three different phenotypes of ULP ICLC in control, NDO (b) and BPS (c) bladders. (**A**) The cytoplasmic actin bundles with densifications (D), short cell processes (arrowheads), many RER cisternae and caveolae (C) are characteristic. (**B**) Mitochondria in the perinuclear area (arrows) and a thin layer of actin filaments in the peripheral cytoplasm (arrowhead) are seen. (**C**) A rather voluminous cytoplasm with mitochondria (M) and RER cisternae are present. Note some densifications in the actin bundles (arrow) and discontinuous basement membrane like material (arrowhead). Scale bars: 1 μm.

Oberkochen, Germany). Images were recorded digitally with a Jenoptik Progress C14 camera system (Jenoptik, Jena, Germany) operated using Image-Pro express software. Analysis was done by an experienced ultrastructural morphologist.

Semi-quantitative analysis

Semi-quantitative analysis was done: measurement of the width of the ULP layer of IC, count of the amount of $CD3^+$ T-lymphocytes in the urothelium, count of the amount of $CD3^+$ T-lymphocytes in the ULP and count of the amount of $CD20^+$ lymphoid aggregates in the lamina propria. All analyses were done blinded on five high-power fields (HPF, 40× magnification) and averaged/ expressed per HPF. For counts of $CD3^+$ T-lymphocytes in the ULP, HPF directly below the urothelium were analysed. Quantitative values are shown as the mean ± S.E. Statistics were performed with Statistica 7.1 (Statsoft, Tulsa, OK, USA). ANOVA test was used to compare the different groups, followed by Fisher *post hoc* tests to define the *P*-values between the groups.

Table 2 Table listing the characteristic ultrastructural features of ICLC in control, NDO and BPS bladders

	Control	NDO	BPS
Aspect	Spindle	Spindle (slender)	Spindle (plump)
Organization	Layers	Layers	Randomly
RER	+++	+++	+++
Caveolae	+++	++	+++
Mitochondria	++	++	++
Actin filaments	Many bundles	Few bundles	Few bundles
EC matrix	Dense	Loose	dense

Results

Phenotype of ULP IC in normal human bladder

When visualized with the light microscope the ULP reveals an IC population that is organized in 10–20 densely packed layers (Fig. 3) and characterized by a vesicular, rather round nucleus and scant eosinophilic cytoplasm. Remarkable regional differences in development of IC were present: within a single section areas of densely packed IC layers alternated with regions that contained only few ULP IC. Ultrastructurally the ULP cells contained caveolae in the peripheral cell membrane and well-developed rough endoplasmic reticulum, mitochondria and peripheral actin filaments (mostly organized in bundles as illustrated by the frequently observed densifications) in the cytoplasm (Figs 1 and 2, Table 2). The cells also showed several discontinuous plasmalemmal thickenings, but no clear fibronexus was seen. Intercellular connections consisted preferentially of intermediate junctions although occasional gap junctions were also observed (data not shown). Immunohistochemical characterization of ULP IC revealed the expression of vimentin, α-sma, podoplanin and CD10 (Figs 3 and 4). Anti-CD10 antibodies only labelled the upper cell layers. This cell

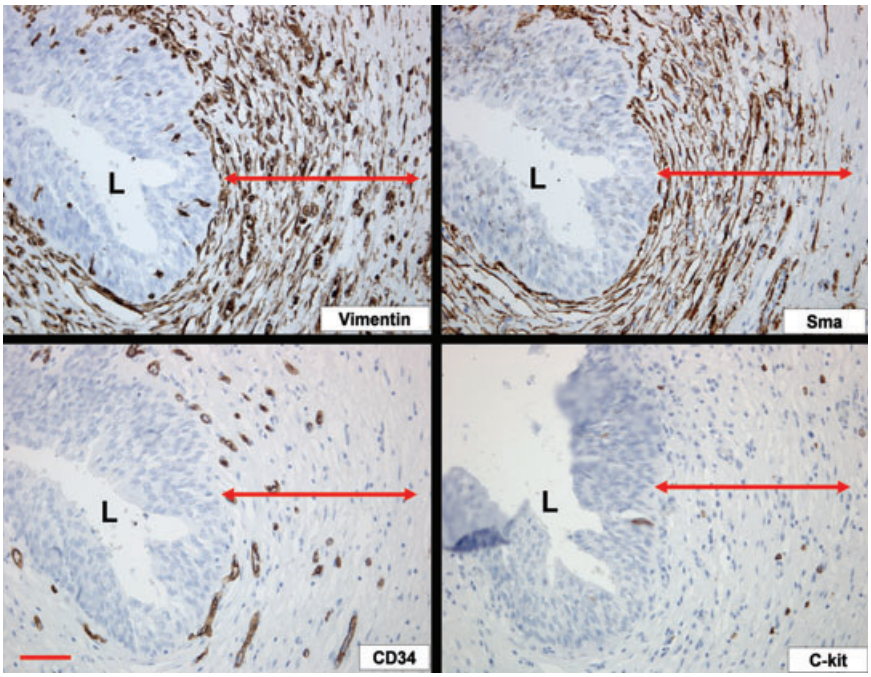

Fig. 3 Figure illustrating the immunohistochemical phenotype of ULP ICLC in control bladder: immunoreactivity for vimentin and α-sma; negativity for CD34 and c-kit. Vimentin is also expressed on blood vessels and nerves. α-sma also stains the perivascular smooth muscle fibres. CD34 stains the ULP blood vessel endothelium. C-kit is expressed on mast cells. Note the organization of ULP ICLC in 10–20 densely packed cell layers, as illustrated by vimentin and α-sma stains. Double arrows mark the ULP ICLC layer. Scale bars: 100 μm. L: lumen.

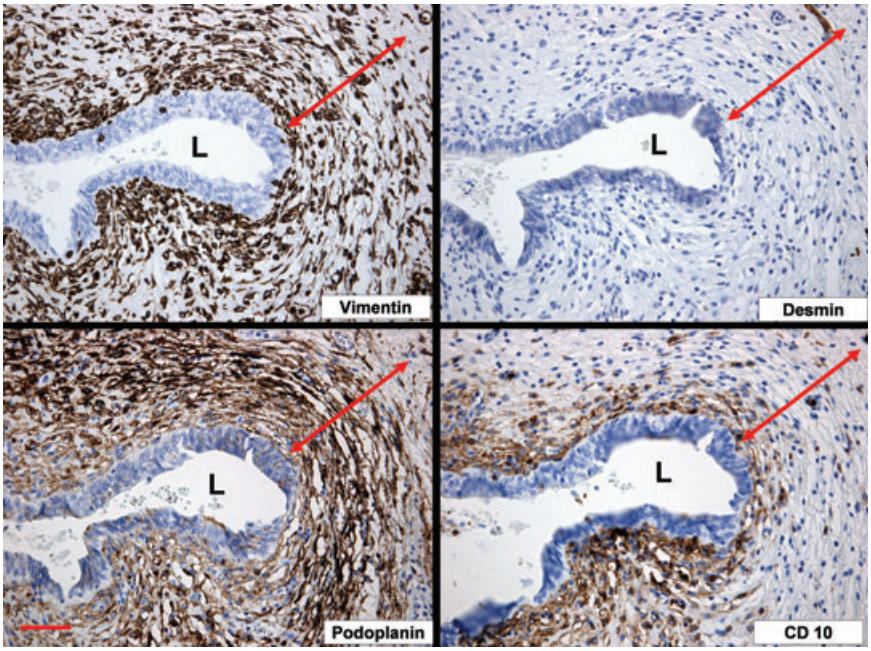

Fig. 4 Figure illustrating the immunohistochemical phenotype of ULP ICLC in control bladder: immunoreactivity for vimentin, podoplanin and partially for CD10; negativity for desmin. Vimentin is also expressed on blood vessels and nerves. Podoplanin stains the lymphatic endothelium. Desmin stains some deeper lying smooth muscle. Double arrows mark the ULP ICLC layer. Scale bars: 100 μm. L: lumen.

population was negative for desmin, CD34 (Figs 3 and 4) and neurofilament (not shown). C-kit-immunoreactivity was clearly detected in several mast cells in the ULP area, as confirmed by a tryptase staining; no clear expression in ULP IC was found (Fig. 5). We cannot exclude the presence of sparse c-kit$^+$ IC in the ULP because a fluorescence double-staining c-kit/tryptase failed, due to technical reasons; nevertheless most c-kit$^+$ cells in the ULP were mast cells in our observations. CD34 expression was found in IC both in the lower parts of the lamina propria (excluding the ULP IC population) as well as in IC between the detrusor smooth muscle bundles. Thus ULP IC constitute a unique cell population expressing vimentin and α-sma, but not desmin nor CD34 (Figs 3 and 6).

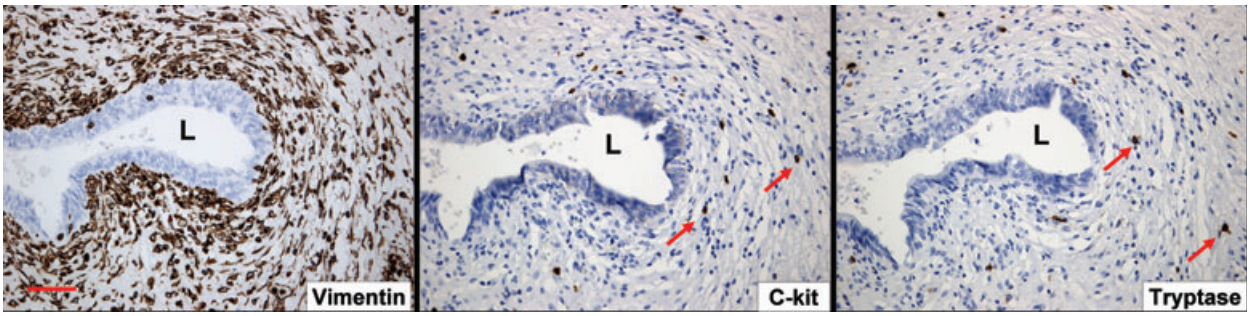

Fig. 5 Figure illustrating the immunohistochemical distribution of c-kit and tryptase in the ULP area in control bladder. Both antigens are expressed on a similar cell population (arrows), which are mast cells. If present on ICLC, then these are very sparsely distributed. Scale bars: 100 μm. L: lumen.

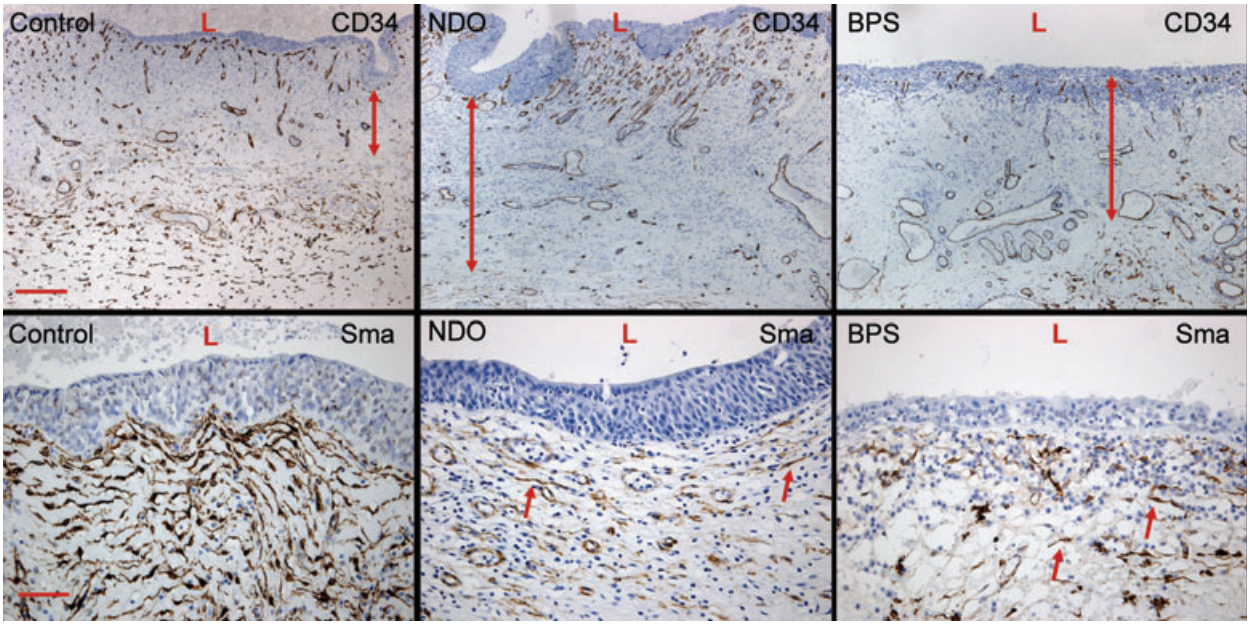

Fig. 6 Upper panels illustrate the increased width of the ULP cell area in NDO bladders, by means of the $CD34^-$ population of ULP ICLC (double arrows). Scale bar equals 200 μm. Lower panels show the decreased α-sma-expression on ULP ICLC (arrows) in both NDO and BPS bladders. Scale bar: 50 μm. L: lumen.

Phenotype of ULP IC in bladder from NDO patients

In bladders from NDO patients ULP IC were still present. However they appeared to be more slender with a broader space in between the cell layers and a less dense intercellular matrix (Fig. 1). Ultrastructurally the IC contained in their cytoplasm less actin filaments (with almost no organization in parallel bundles) and less caveolae in their peripheral membrane compared to those in normal bladders. In the perinuclear area several mitochondria and well-developed rough endoplasmic reticulum cisternae were obvious (Fig. 2). The immunohistochemical phenotype differed slightly: the IC were still $vimentin^+$ but tend to express less α-sma (in line with the ultrastructural data, observed in all NDO bladders) (Fig. 7). Quantification of the reduced number of $\alpha\text{-soma}^+$ IC was difficult because the ULP area of IC was significantly enlarged in NDO bladders (Table 3, Fig. 6) (which means that comparison of cell counts/area with normal bladders was problematic). The ULP IC were also still immunoreactive for podoplanin and CD10 and negative for desmin and CD34. A significantly higher amount of $CD20^+$ lymphoid aggregates/HPF compared to control bladders was present in the lamina propria of NDO bladders (Fig. 7, Table 3). The amounts of $CD3^+$ T cells/HPF in the urothelium and in the ULP were not significantly increased compared to controls. A remarkable

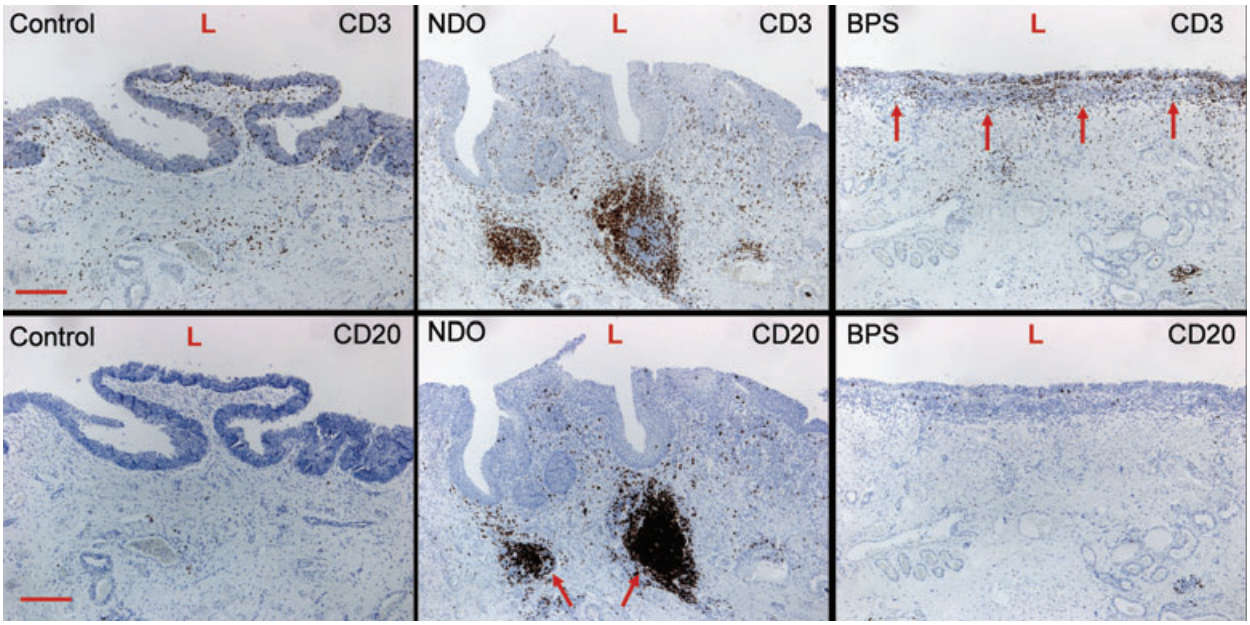

Fig. 7 Upper panels illustrate the significant increase in $CD3^+$ lymphocytes in the urothelium and ULP area of BPS bladders (arrows). Lower panels indicate the significant increase in $CD20^+$ lymphoid aggregates in the bladder lamina propria of NDO bladders (arrows). Scale bars: 50 μm. L: lumen.

Table 3 Table showing the semi-quantitative analysis of several parameters in control, NDO and BPS bladders

	Control	MS	BPS
Width ULP IC area(μm)	0.25 ± 0.06	**0.86 ± 0.19**	0.54 ± 0.13
T cells in urothelium/HPF	12.17 ± 2.22	12.80 ± 1.91	**26.68 ± 3.75**
T cells in ULP/HPF	47.00 ± 8.68	73.83 ± 7.18	**111.5 ± 17.05**
Lymphoid aggregates in lamina propria/HPF	0.25 ± 0.15	**0.87 ± 0.13**	0.60 ± 0.18

Values are expressed as means ± S.E. Values in bold are significant compared to controls (*P*-values < 0.05). EC: extracellular.

observation on electron microscopy was the close apposition of lymphocytes to IC in the ULP, lying in the same direction, and thus creating couples of IC and lymphocytes (Fig. 1).

Phenotype of ULP IC in bladder from BPS patients

In bladders from BPS patients a remarkable loss of organization in layers of ULP IC was noticed (Fig. 1). Furthermore there was a heterogeneous population of interlaying inflammatory cells: lymphocytes, mast cells, plasma cells and macrophages (Fig. 1). Ultrastructurally the IC contained in their cytoplasm actin filaments with densifications and caveolae at the peripheral cell membrane, in a smaller amount as compared to those in normal bladders. Several mitochondria and many rough endoplasmic reticulum cisternae were present (Fig. 2). The close apposition of lymphocytes on IC, as observed in bladders form NDO patients, was not as obvious. The immunohistochemical phenotype was preserved: immunoreactivity for vimentin, α-sma, podoplanin and CD10; no staining with antibodies directed to desmin, CD34, neurofilament and synatophysin. A trend towards decreased amount of α-sma^+ IC was also observed, however less pronounced as in NDO bladders. Only few $c\text{-}kit^+$ cells were present. The numbers of $CD3^+$ T cells/HPF in the urothelium and in the ULP were significantly increased compared to controls ($P < 0.05$, Fig. 7, Table 3). No higher numbers of $CD20^+$ lymphoid aggregates/HPF compared to control bladders were present in the lamina propria of NDO bladders (Fig. 8, Table 2). Another observation was the focal presence of urothelial denudation in all BPS bladders.

Discussion

Wiseman *et al.* were the first to describe in detail the ultrastructure of the ULP layer of IC, which they categorized as myofibroblasts [8]. Others have questioned this myofibroblast phenotype due to

the absence of fibronexus; instead they proposed a smooth muscle phenotype [10, 11]. In the present study we have tried to further clarify the phenotype of these cells using electron microscopy as the golden standard technique, associated with a large panel of immunohistochemical stains. The main ultrastructural features of the ULP IC are abundant RER, many actin filaments with densifications, multiple caveolae, well-developed Golgi apparatus, several mitochondria and intercellular contacts (intermediate junctions and gap junctions). These cells are immunoreactive for vimentin, α-sma, podoplanin and CD10 (superficial layers) and did not stain with antibodies directed to CD34, desmin, c-kit, synaptophysin and neurofilament.

The ultrastructural phenotype found in the present study is highly similar to that reported by others [8]. However a straightforward classification is not so obvious. Features that do not match with the classical ICC are the presence of abundant RER, the numerous actin filaments and the lack of immunoreactivity with antibodies to c-kit and to CD34 [12]. Arguments against myofibroblast phenotype are the absence of fibronexus and the presence of caveolae [10, 11]. The archetypical smooth muscle phenotype is also unlikely due to the abundant presence of RER and the immunohistochemical negativity for desmin. In the literature this problem with phenotyping is not new, and several authors have reported on the presence of a spectrum of spindle cell phenotypes, bearing to greater or lesser extent the ultrastructural features of myofibroblast, ICC, fibroblast or smooth muscle cell [10, 12]. Putting together all morphological and immunohistochemical data we conclude that the phenotype of the main population of ULP IC lies somewhere in between that of a typical ICC and a typical myofibroblast, having features of both. Therefore we classify these cells as ICLC, a terminology which has been proposed before [13, 14].

We were unable to demonstrate c-kit on ULP ICLC: the few c-kit$^+$ cells appeared to be all mast cells given the similar staining pattern for tryptase. Literature on c-kit expression in bladder ICLC shows conflicting reports: publications mentioning c-kit on ICC [15–17] alternate with papers that state the opposite [18, 19]. Almost no study on the expression of c-kit on bladder ULP ICLC used tryptase staining as a control for mast cells, which at least in our hands shows an almost full overlap. A recent paper mentioned the presence of c-kit$^+$/tryptase + ICC in the lamina propria [17]. This report however deals with IC throughout the lamina propria, whereas our study was focused on ICLC directly beneath the urothelium (= ULP) which are – in our hands – negative for c-kit.

The function of ULP ICLC has been under debate for several years. Because these cells are closely packed together underneath the urothelium, with intercellular connections and a distinct phenotype from the stromal cells covering the major part of the lamina propria, it is likely that these cells play a specific role in bladder physiology. Due to their localization, a communicating role between urothelium and detrusor and/or afferent nerves could be possible. A remarkable observation was the changing densities of ULP ICLC in a single biopsy, which could also have functional implications. Future studies should focus on the expression of specific ion channels or membrane receptors (such as TRP channels [20]), which are likely to give more insight into the function of this cell layer. The significance of CD10- and podoplanin immunoreactivity of ULP ICLC remains to be determined. Both markers have been studied on fibroblasts in the stroma surrounding tumour nests. Podoplanin was found to be up-regulated in cancer associated fibroblasts, both in colorectal [21] and lung [22] adenocarcinomas. CD10 expression in tumour-associated stromal cells has been described in several tumours [23–25]. Both markers could be related to a myofibroblast phenotype, because myofibroblasts are more and more seen as activated mesenchymal cells in tumour or inflammatory conditions [10]. In bladder both CD10 and podoplanin have a similar immunohistochemical expression pattern on ULP ICLC in normal and inflammatory conditions. However future quantitative studies might reveal differences in expression in pathologic conditions.

The ultrastructural and immunohistochemical phenotype of ULP ICLC showed modest changes in the pathologic conditions studied. In NDO bladders ULP ICLC showed less actin filaments together with a decreased expression of α-sma and also less caveolae. This observation suggests a trend towards a fibroblast phenotype. Furthermore the ULP area of ICLC was significantly broadened in NDO bladders with a remarkable less dense intercellular matrix and a broadened space between cell layers. These findings might also be due to a changed phenotype of the ULP ICLC. The functional implications of these observations remain to be determined, but it is likely that these are some of the many elements contributing to altered bladder function in NDO patients [26]. Also in bladders from BPS-patients the phenotype of the ULP ICLC showed a slight shift towards a fibroblast phenotype. The organization in dense parallel layers was clearly disturbed, resulting in a chaotic organized group of ICLC. The functional significance of these observations remains also unclear.

A remarkable finding was the enhanced inflammatory response in both NDO and BPS bladders, clearly with different characteristics. In NDO bladders frequent close apposition of lymphocytes and ULP ICLC was found, which might indicate a role of ICLC in antigen-presentation to T cells. Furthermore a significantly increased number of CD20$^+$ lymphoid follicles were found in the lamina propria of these bladders. In BPS bladders a dense infiltrate of CD3$^+$ lymphocytes was found in the area of ULP ICLC. This finding was clearly less pronounced in NDO bladders. The particular apposition of CD3$^+$ T-lymphocytes to ULP ICLC was not found. The inflammatory infiltrate here was denser and more heterogeneous with plasma cells and mast cells. An increased number of inflammatory cells in bladder mucosa, especially T cells, have been reported before [27, 28]. It is however remarkable that this field is relatively unexplored. The further exploration of the functional significance of lamina propria inflammation in NDO and BPS is beyond the scope of this study, but the abundant presence of T cells in NDO and BPS bladders, both with a different presentation is likely to influence the physiological role of the ULP ICLC cell layer. Whether this inflammatory response is a primary or secondary phenomenon needs to be elucidated.

In conclusion we have defined the ULP IC as ICLC, with an ultrastructural an immunohistochemical phenotype somewhere between that of an archetypical myofibroblast and ICC. We further found obvious changes in the phenotype and/or topographical organization of these cells in NDO and BPS bladders, with a shift towards a fibroblast phenotype in both diseases. A remarkable high number of lymphocytes were found in the area of ULP ICLC, with a different topographical pattern in NDO and BPS bladders. Future studies should focus on specific receptor and ion channel expression profiles of these cells to elucidate the functional role of this intriguing cell layer in both normal and pathological bladders. Microdissection of this layer might therefore be a valuable experimental tool.

Acknowledgement

We are grateful to Paula Aertsen, Lieve Ophalvens, Rolande Renwart and Chris Armee for the excellent technical support. Dirk De Ridder is a fundamental-clinical researcher at the FWO-Vlaanderen. This research was funded by FWO-Vlaanderen G.0419.03.

Conflict of interest

The authors confirm that there are no conflicts of interest.

References

1. **de Groat WC.** A neurologic basis for the overactive bladder. *Urology*. 1997; 50: 36–52.
2. **Drake MJ, Mills IW, Gillespie JI.** Model of peripheral autonomous modules and a myovesical plexus in normal and overactive bladder function. *Lancet*. 2001; 358: 401–3.
3. **Blyweert W, Van Der Aa F, Ost D, *et al*.** Interstitial cells of the bladder: the missing link? *Bjog*. 2004; 111: 57–60.
4. **McCloskey KD.** Interstitial cells in the urinary bladder – localization and function. *Neurourol Urodyn*. 2010; 29: 82–7.
5. **Lang RJ, Klemm MF.** Interstitial cell of Cajal-like cells in the upper urinary tract. *J Cell Mol Med*. 2005; 9: 543–56.
6. **Fry CH, Sui GP, Kanai AJ, *et al*.** The function of suburothelial myofibroblasts in the bladder. *Neurourol Urodyn*. 2007; 26: 914–9.
7. **Davidson RA, McCloskey KD.** Morphology and localization of interstitial cells in the guinea pig bladder: structural relationships with smooth muscle and neurons. *J Urol*. 2005; 173: 1385–90.
8. **Wiseman OJ, Fowler CJ, Landon DN.** The role of the human bladder lamina propria myofibroblast. *BJU Int*. 2003; 91: 89–93.
9. **Kuijpers KA, Heesakkers JP, Jansen CF, *et al*.** Cadherin-11 is expressed in detrusor smooth muscle cells and myofibroblasts of normal human bladder. *Eur Urol*. 2007; 52: 1213–21.
10. **Eyden B.** The myofibroblast: phenotypic characterization as a prerequisite to understanding its functions in translational medicine. *J Cell Mol Med*. 2008; 12: 22–37.
11. **Eyden B.** Are there myofibroblasts in normal bladder? *Eur Urol*. 2009; 56: 427–9.
12. **Pieri L, Vannucchi MG, Faussone-Pellegrini MS.** Histochemical and ultrastructural characteristics of an interstitial cell type different from ICC and resident in the muscle coat of human gut. *J Cell Mol Med*. 2008; 12: 1944–55.
13. **Drake MJ, Fry CH, Eyden B.** Structural characterization of myofibroblasts in the bladder. *BJU Int*. 2006; 97: 29–32.
14. **Popescu LM, Faussone-Pellegrini MS.** TELOCYTES – a case of serendipity: the winding way from interstitial cells of Cajal (ICC), *via* interstitial Cajal-like cells (ICLC) to TELOCYTES. *J Cell Mol Med*. 2010; 14: 729–40.
15. **Shafik A, El-Sibai O, Shafik AA, *et al*.** Identification of interstitial cells of Cajal in human urinary bladder: concept of vesical pacemaker. *Urology*. 2004; 64: 809–13.
16. **Van Der Aa F, Roskams T, Blyweert W, *et al*.** Identification of kit positive cells in the human urinary tract. *J Urol*. 2004; 171: 2492–6.
17. **Johnston L, Woolsey S, Cunningham RM, *et al*.** Morphological expression of KIT positive interstitial cells of cajal in human bladder. *J Urol*. 2010; 184: 370–7.
18. **Rasmussen H, Rumessen JJ, Hansen A, *et al*.** Ultrastructure of Cajal-like interstitial cells in the human detrusor. *Cell Tissue Res*. 2009; 335: 517–27.
19. **Gillespie JI, Markerink-van Ittersum M, de Vente J.** Expression of neuronal nitric oxide synthase (nNOS) and nitric-oxide-induced changes in cGMP in the urothelial layer of the guinea pig bladder. *Cell Tissue Res*. 2005; 321: 341–51.
20. **Everaerts W, Gevaert T, Nilius B, *et al*.** On the origin of bladder sensing: tr(i)ps in urology. *Neurourol Urodyn*. 2008; 27: 264–73.
21. **Yamanashi T, Nakanishi Y, Fujii G, *et al*.** Podoplanin expression identified in stromal fibroblasts as a favorable prognostic marker in patients with colorectal carcinoma. *Oncology*. 2009; 77: 53–62.
22. **Kawase A, Ishii G, Nagai K, *et al*.** Podoplanin expression by cancer associated fibroblasts predicts poor prognosis of lung adenocarcinoma. *Int J Cancer*. 2008; 123: 1053–9.
23. **Nishihara Y, Aishima S, Hayashi A, *et al*.** CD10+ fibroblasts are more involved in the progression of hilar/extrahepatic cholangiocarcinoma than of peripheral intrahepatic cholangiocarcinoma. *Histopathology*. 2009; 55: 423–31.
24. **Iwaya K, Ogawa H, Izumi M, *et al*.** Stromal expression of CD10 in invasive breast carcinoma: a new predictor of clinical outcome. *Virchows Arch*. 2002; 440: 589–93.
25. **Ogawa H, Iwaya K, Izumi M, *et al*.** Expression of CD10 by stromal cells during colorectal tumor development. *Hum Pathol*. 2002; 33: 806–11.
26. **Ciancio SJ, Mutchnik SE, Rivera VM, *et al*.** Urodynamic pattern changes in multiple sclerosis. *Urology*. 2001; 57: 239–45.
27. **Thilagarajah R, Witherow RO, Walker MM.** Quantitative histopathology can aid diagnosis in painful bladder syndrome. *J Clin Pathol*. 1998; 51: 211–4.
28. **Christmas TJ.** Lymphocyte sub-populations in the bladder wall in normal bladder, bacterial cystitis and interstitial cystitis. *Br J Urol*. 1994; 73: 508–15.